CROSS SECTIONS FOR PRODUCING MOLECULAR IONS FROM METHANE FOR FAST F, Si, AND C PROJECTILES

by

NABIL B. MALHI

B.S., UNIVERSITY OF JORDAN, AMMAN/ JORDAN, 1980

M.S., UNIVERSITY OF JORDAN, AMMAN/ JORDAN, 1982

A MASTER'S THESIS

submitted in partial fulfillment of the

requirements for the degree

MASTER OF SCIENCE

Department of Physics

Kansas State University

1986

Approved by

Major Professor

TABLE OF CONTENTS

LIST OF FIGURES

Figure Page

LIST OF TABLES

ACKNOWLEDGMENT

I would like to express my most sincere gratitude to Professor Tom J. Gray for his guidance and encouragement throughout the cource of this work.

I wish to express my sincere appreciation to Professor James Legg for his generous help and guidance in the cource of this work.

I would like to thank Professor J. McGuire for the valuable discussion on the theoretical aspect of this work.

I extend thanks to my committee member Dr. Talat Rahman for her valuable comments and suggestions concerning the content of this work.

I would like to acknowledge the help and friendship of Vince Needham and Kevin Carnes during the cource of this work.

I am gratefull to the accelerator's staff through their supervisors R. Krause, D. Hill, and M. Ross.

I acknowledge the financial support of the U.S Department of energy, and the Arideast.

CHAPTER ONE

INTRODUCTION

Since 1960 when studies on the collisions of MeV atomic ions with atoms and molecules have been conducted, the ion-molecule collision in gases became a subject of interest. Studies of ion-molecule collision in a high energy range can improve the understanding of the earth's atmosphere as well as the formation and destruction processes for the interstellar molecules.

Collision between fast positive ions and gas atoms or molecules are responsible for the detachment of electrons from either or both of the colliding particles. C.L.Cocke[1] first reported the study of low velocity highly charged Ar recoil ion production for fast Cl ions incident upon an Ar target gas. Other studies followed[2-4] which were additional investigations of recoil ion production by fast heavy ions. This and other processes lead to the formation of singly-charged and multiply-charged recoil target ions.

Until the present work, no published measurements of the formation cross-sections of the molecular recoil ions produced from light molecules ($M \leq 20$) as a result of

collisions evolving heavy ions have been carried out.

This work addresses the measurement of the formation cross-sections of singly-charged (CH_4^+ , CH_3^+ , CH_2^+ , CH^+ , C^+) and doubly-charged (CH_2^{2+} , CH^{2+} , C^{2+}) recoil ions, from CH_4 after being bombarded with 1 MeV/amu F^{q+}, Si^{q+} and C^{q+} projectiles. The projectile initial charge state, and projectile atomic number dependences for molecular ion production were investigated.

This thesis is divided into five chapters. The first chapter is an introduction, the second chapter will be devoted to a review of some of the previously published work that been directed to the study of the formation of molecular ions from methane. In chapter three, the experimental apparatus and procedures are presented. Chapter four, presents the data analysis and results. In chapter five, the summary and conclusions of this work are presented.

CHAPTER TWO

BACKGROUND

It has been shown[1] that in a single collision when a fast highly charged ion is in collision with a neutral target species it may, with a large probability, eject a number of the target electrons without imparting much energy to the target center of mass. A collision sufficiently violent to produce inner-shell exitation has been shown[5] experimentally to be still gentle enough for the production of slow moving recoil ions.

The first direct observation of low velocity heavy ions produced from the bombardment of targets by fast heavy ions ($\gtrsim$MeV/amu) was reported by Macfarlane and Torgerson.[6] Following this work Edwards, et al.[7] reported the direct observation of charged molecular fragments as a result of the dissociation of diatomic molecules by 1 MeV H^+ and He^+ ions.

The dissociation of methane has been studied since 1936 when Smith[8] reported the first series of mass-spectrometry studies of the product of ionization of polyatomic molecules by low velocity electrons. Since that time most of the

effort has been concentrated on the determination of appearence potentials and the measurement of the relative abundances of different kinds of ions produced by electron bombardment of polyatomic molecules. Since CH_4 is the simplest hydrocarbons it was a subject of a great number of studies in mass-spectrometry. The validity of Born approximation for molecular fragmentation from methane was studied by Wexler[9] when he bombarded CH_4 gas with sufficiently high energy electrons and protons of the same velocity. An interesting review of the investigation of the fragmentation of CH_4 by various types of ionizing beams was done by Reed.[10] Cross-sections for the production of singly-charged molecular ions from CH_4 by electrons bombardment (from 20 to 2000 eV) was done by Adamczyk, et al.[11] No metastable multiply-charged molecular ions from methane have been directly observed when using an electron as the projectile. Doubly charged CH_4^{2+} ions first observed by Spohr, et al.[12] using the ESCA technique. Using charge stripping reactions Ast, et al.[13] were able to observe CH_4^{2+}. The observation of CH_2^{2+} and C^{2+} resulting from the decay of CH_4^{2+} were observed by Rabrenovic, et al.[14]. Using the time-of-flight technique for the ions formed in a gas cell filled with CH_4 Gray, et al.[15] were able to make the first direct observation of CH^{2+} metastable recoil ion and indirect observations of CH_3^{2+} metastable ions.

CHAPTER THREE

EXPERIMENT

[A]Experimental Apparatus :

Negative ions were extracted from the sputter or the diode source and accelerated by the model EN 6 MV tandem Van de Graaff accelerator at the James R. Macdonald laboratory, Kansas State University. A schematic diagram of the tandem Van de Graaff accelerator is shown in figure 1. The Negative ions were selected according to their momenta by a 20° inflection magnet and accelerated to the high voltage terminal set to the proper voltage to give the ions the required energy. Electrons from the negative ions were stripped off by a gas stripper at the terminal, and emerge in various positive charge states. Positive ions with different charge states were accelerated away from the terminal giving different energies depending on the charge state of the positive ion, this energy is of the form

$$E = (1+q)V$$

where E is the ion energy, q is the final ion charge state,and V is the accelerator terminal voltage. The high energy ion beam is directed into the 90° analyzing magnet where the ions with the required energy, mass, and charge

state were selected according to the rigidity, $\sqrt{\frac{mE}{q^2}}$. The present measurements required high energy ions with different charge states and the same energy. A thin carbon foil post stripper was placed between the analyzing magnet and the switching magnet. After passing through the post stripper foil the ion beam is represented by an essentially gaussian charge state distribution. Ions with the desired charge state can then be selected by the switching magnet and be directed onto the target for the measurements of the molecular ion production cross-sections.

Since the purpose of this experiment is to measure the production cross-sections for molecular ions from methane in a single collision, the pressure need to be maintained at low value. The pressure in the target gas cell, through which the fast heavy ion beam passes, was monitored by means of a capacitance manometer. A constant target pressure was maintained by using a manually controlled leak valve. The target gas was maintained at pressure usually between 0.1 and 0.5 mTorr. The background pressure of the vacuum chamber was maintained at about 5×10^{-7} Torr.

Molecular ions are generated when collisions between the incident heavy ion beam and the target gas inside a recoil ion source takes place. The development and application of recoil ion sources is reviewed by Gray and

Figure 1: A schematic diagram of the Kansas State university 6 MV tandem Van de Graaff.

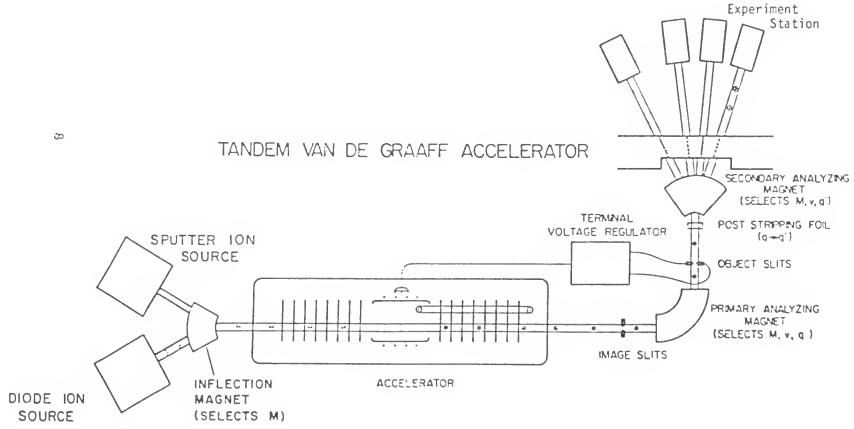
TANDEM VAN DE GRAAFF ACCELERATOR
Experiment Station
SECONDARY ANALYZING MAGNET (SELECTS M, v, q)
POST STRIPPING FOIL (q→q')
OBJECT SLITS
TERMINAL VOLTAGE REGULATOR
PRIMARY ANALYZING MAGNET (SELECTS M, v, q)
IMAGE SLITS
SPUTTER ION SOURCE
DIODE ION SOURCE
INFLECTION MAGNET (SELECTS M)
ACCELERATOR

Cocke.[16] The recoil ion source used in this work is shown in figure 2. It consists of three grids, the pusher at potential V_1, the foucusing electrode at potential V_2 ($V_1 > V_2$) and the third grid is at ground potential. The potentials V_1 and V_2 were typically at +1000 and +965 volts respectively. An electric field at right angles to the extracted recoil ions could be applied to steer them outside the cell by two sets of deflectors. The recoil ions then drift a distance of about 7 cm before entering a 180° magnetic spectrometer of focal length 7 cm . The ions passed by the magnetic spectrometer are detected by a channel plate detector a distance of about 7 cm away from the exit of the magnet, see figure 2. Typical spectrum for a scan of the M/q region containing the molecular ions of interest is given in figures 3 and 4.

To reduce interference from impurity ions in the spectra, a methane gas of purity 99.99% was used. To check for any residual gases in the chamber, a background spectrum was collected, which shows that M/q=8 is totally O^{2+}, but not CH_4^{2+} . The percentage abundance of the ^{13}C contaminant isotope is 1.11% of ^{12}C , the ratio of CH^+/C^+ and CH^{2+}/C^{2+} were considered to check for the $^{13}C^+$ and $^{13}C^{2+}$ appearance. The Coulomb explosion of N^{2+} insure that observed peaks at M/q=7 is CH_2^{2+} not N^{2+}. Consider the case

Figure 2: Experimental apparatus with detail of the recoil ion source.

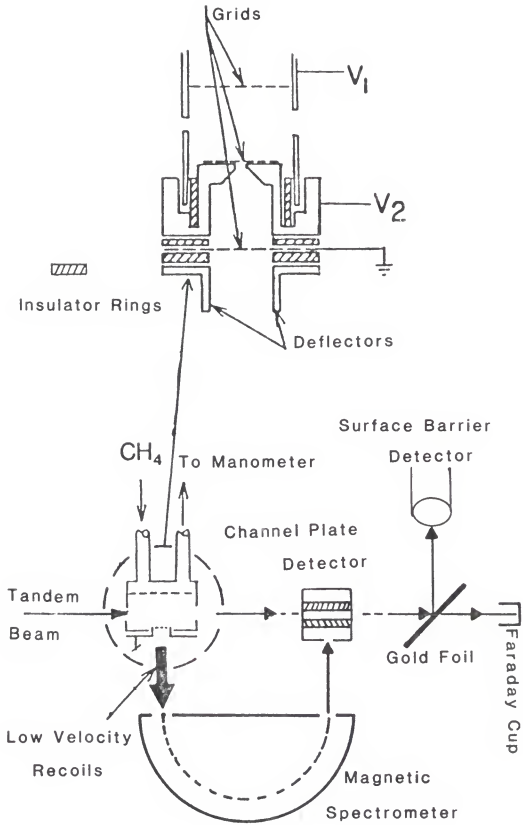
Grids
V_1
V_2
Insulator Rings
Deflectors
Surface Barrier
Detector
CH_4
To Manometer
Channel Plate
Detector
Tandem
Beam
Gold Foil
Faraday Cup
Low Velocity
Recoils
Magnetic
Spectrometer

Figure 3: Typical spectrum of singly-charged molecular ions from methane.

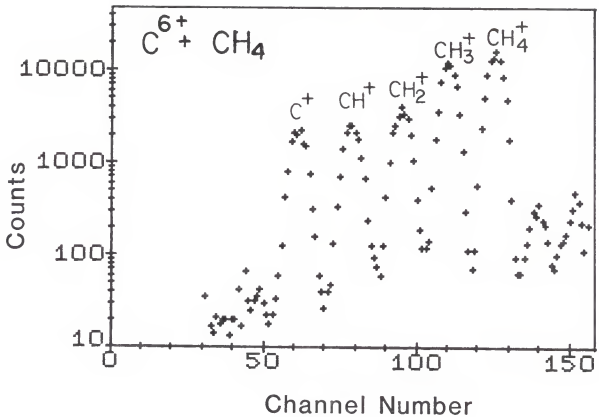
C^{6+} + CH_4
C^+
CH^+
CH_2^+
CH_3^+
CH_4^+
10000
1000
100
10
Counts
0
50
100
150
Channel Number

Figure 4: Typical spectrum of doubly-charged molecular ions from methane, with M/q= 6, 6.5, 7, and 8 are C^{2+} , CH^{2+} + $^{13}C^{2+}$, CH_2^{2+} and O^{2+} respectively.

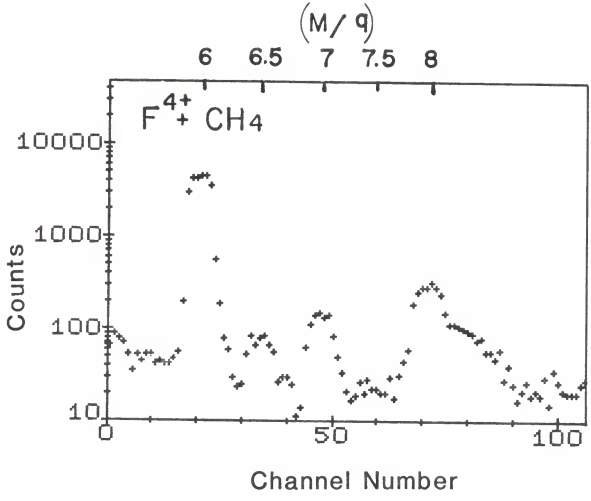
(M/q)
6
6.5
7
7.5
8
F^{4+} + CH_4
10000
1000
100
10
Counts
0
50
100
Channel Number

for a fast heavy ion incident upon a diatomic molecule. Our observations in an experimental configuration as described by Needham[17] for the resulting atomic ion fragments of a diatomic molecule are shown diagramatically in figure 5 for 19 MeV F^{4+} incident upon N_2. Similar results have been measured for both O_2 and CO_2 target gases.

In figure 5 the arrow indicates the position of the N^{2+} atomic ion that would result from $F^{4+} + N_2 \longrightarrow N^{2+} + N$. We observe no intensity at this position (the arrow) in the 2-dimensional spectrum illustrated in figure 5.

A projection of the intensities for the left and right lobes in figure 5 would produce a double peak structure in the magnet scan spectra of this work. At M/q=7 we observe no such double peak structure but only single sharp peaks. This means that our observations above ensure that M/q=7 is CH_2^{2+} and not N^{2+}.

Normalization of the data for different incident ions was achieved using Rutherford scattering of the beam by a thin gold target placed after the target region. The scattered heavy ions were detected at 90° with respect to the beam direction. The data in each channel of the spectrum shown in figures 3 and 4 was collected for a predetermined number of events detected by the Rutherford scattering

Figure 5 : A schematic diagram of the resulting atomic ion fragments of the diatomic molecule N_2.

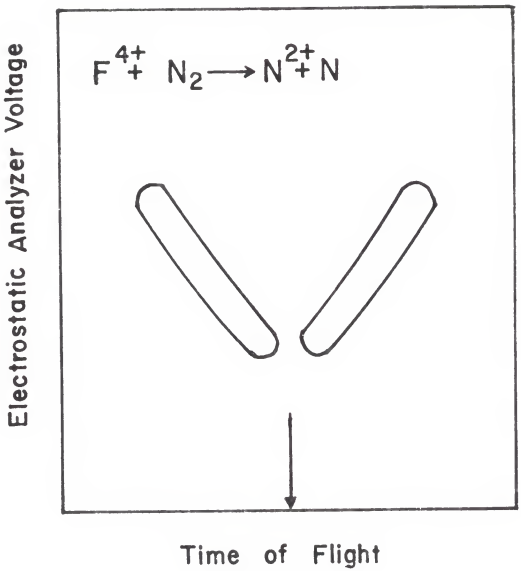
$F^{4+} + N_2 \longrightarrow N^{2+} + N$
Electrostatic Analyzer Voltage
Time of Flight

detector. A surface barrier detector was used to detect the scattered heavy ions.

The electronics set up is shown as a block diagram in figure 6. The purpose of this set up is to scan the recoil ions for different projectiles. The scan is performed by a magnetic spectrometer, where its coil current is stepped by a programable power supply which is controlled by a program developed at Kansas State university to drive a CAMAC module Digital-to-Analog convertor (DAC). The output of the DAC provides the current control signal for the magnet current. The scanning procedures are as follows:

(a) The surface barrier detector, which counts the beam particles, sends a signal for this beam flux to the Up-Down (UP-DN) counter to count down for the desired Q-counts/channel, which is set by the program.

(b) At the same time while the UP-DN counter is counting, the scanned recoil ion is transmitted through the spectrometer which is set at the selected current; this transmitted ion is detected by a channel plate detector from which a signal is sent to a constant fraction discriminator (CFD) module, a fast signal out of this module is sent to the HEX scalar, from which sends a signal to the PDP-11/34 computer.

Figure 6 : A schematic of electronics used for the analyzing system.

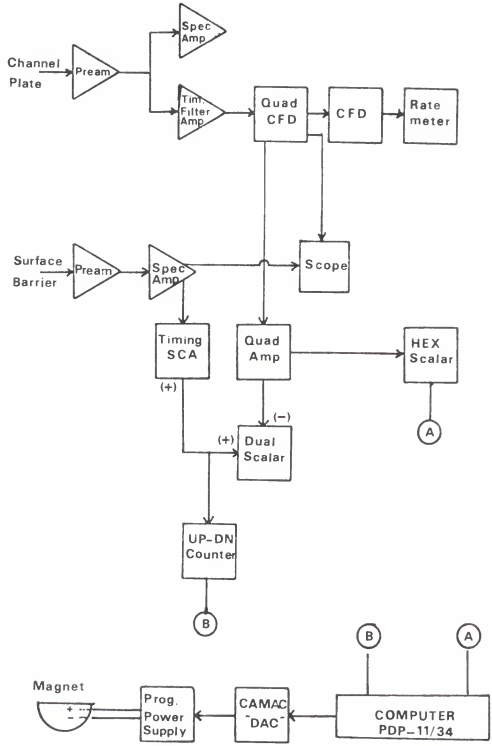
Channel Plate
Preamp
Spec Amp
Tim. Filter Amp
Quad CFD
CFD
Rate meter
Surface Barrier
Preamp
Spec Amp
Scope
Timing SCA
Quad Amp
HEX Scalar
(+)
(−)
(+)
Dual Scalar
A
UP-DN Counter
B
B
A
Magnet
Prog. Power Supply
CAMAC DAC
COMPUTER PDP-11/34

(c) After the UP-DN counter finishes counting the desired Q-counts/channel, a signal is sent to the computer, and this channel which is sent by the HEX scaler to the computer, is stored in the multichannel analyser.

(d) Then the computer will send a digital signal to the DAC, this signal will be sent to the power supply which in turn steps in the voltage applied to the magnet coil for the scanning of the next channel, and so on.

[3]Experimental Procedures:

In order to perform the measurements of recoil ion production cross-sections, several important consideration were carefully examined. These included:

1)Recoil ion source, magnetic spectrometer and detector alignment.

2)Reproducibility of the experiment.

3)Statistics, or counts taken for each channel of the spectrum.

4)Pressure dependence.

5)counting dead time corrections and minimization.

The alignment of the experimental apparatus was done using a small laser source and a 45° mirror as follows:

a) The recoil ion source was aligned with the beam line using the telescope.

b) Then the entrance of the magnet was aligned with the exit of the recoil ion source, by passing the reflected laser beam, which was reflected from the surface of the 45° mirror in a right angle, through the focal point of the entrance of the magnet,then to the exit of the recoil ion source.

c) Then the exit of the magnet (main radius) was aligned with the channel plate detector by shining the laser beam through the magnet exit to the channel plate detector entrance.

Now concerning the reproducibility: while the switching magnet (S.M.) was set at the optimum beam position, we did a scan of a spectrum and measured the integrated peak intensities. Then the position of the S.M. was changed right and left to cut the beam current, this change resulted in a change in the spectrum integral by about 40% or more. The same test was done with the vertical high energy

steerers and the einzel lens which resulted also in a high change in the spectrum integral. To get rid of this problem, or to have an experimental results which are independent of beam fluctuation, the two set of slits in front of the chamber were aligned with the recoil ion source, the opening of the slits were much smaller than the width of the recoil ion source entrance apperture. It was found that the resolution for a peak was strongly affected by the height of the slit opening,so to improve the resolution, decrease vertical height of slit opening was needed. With this alignment we were able to get a reproducibility of about 10% or better, independent of input beam position.

In order to get good statistics for each spectrum we were careful about having the area under the smallest peak of the singly-charged recoil ions spectrum of about 10K counts, and about 2K counts for the doubly-charged one. With the channel plate detector's grid potential at +400 volts and the plates each at -950 volts we were able to get a resolution of about 100:1 peak to valley ratio. Figure 3 shows this resolution.

The intensity of primary recoil ions should increase linearly with the pressure, P, under single collision conditions. whereas that of an ion formed by a multiple collision would increase as P^2 or higher. Figure 7 and 8 show the yield of a singly-charged recoil ions produced from methane as a function of the gas cell pressure, the curves appear to be linear below 0.43 mT. Cross-section measurements were all made at pressure below o.43 mT.

The system dead time was increased by increasing the beam current. It was found that for a beam current >1 nA there is about 50% dead time correction for the highest peak in the spectrum, were we noticed that the dead time increases with increasing the counting rate in the peak. A dead time correction of about 5% was achieved by lowering the beam current and by using a fast electronics for the signal.

Figures 7&8 : The yield of the singly-charged recoil ions produced from methane as a function of the gas cell pressure.

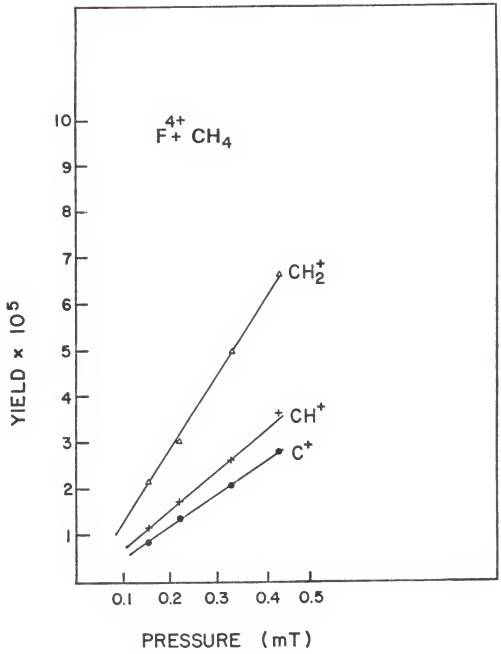
$F^{4+} + CH_4$
CH_2^+
CH^+
C^+
YIELD x 10^5
PRESSURE (mT)
1
2
3
4
5
6
7
8
9
10
0.1
0.2
0.3
0.4
0.5

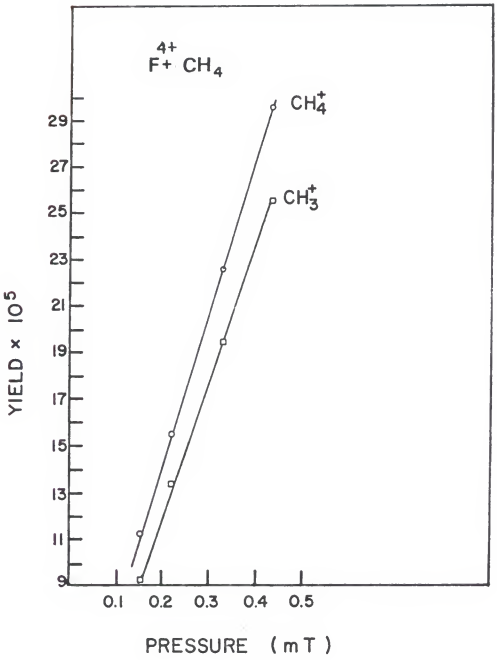
4+
F+ CH4
CH4+
CH3+
YIELD x 10^5
29
27
25
23
21
19
17
15
13
11
9
0.1
0.2
0.3
0.4
0.5
PRESSURE (mT)

CHAPTER FOUR

DATA ANALYSIS AND RESULTS

As beam passes through the target gas the yield of the molecular recoil ions $Y_{m,q}$ is given by:

$$Y_{m,q} = \Phi_I \, \bar{\sigma}_{m,q} \, N \varepsilon \, d\Omega , \qquad (1)$$

where, Φ_I represents the total number of incident particles, N is the target density (thickness of the gas target) in molecules/cm^2, ε is the detection efficiency, $d\Omega$ is the solid angle of detection and $\bar{\sigma}_{m,q}$ is the molecular recoil ion production cross-section for recoil ions with mass m and charge state q.

By means of the ideal gas equation, we can relate the thickness of the gas target to the pressure within the gas cell in the following equation:

$$N = N_A \frac{P \, L}{R \, T} \qquad (\text{molecules/cm}^2) \qquad (2)$$

where, N_A=6.025x10^{23}molecules/mole (Avogadro's number), P is the target gas pressure in units of mTorr, L is the cell length in cm, R is the universal gas constant and T is the temperature of the target in unit of $^{\circ}$K.

For one mole $RT_o = PV$, and at STP P=760 mmHg (760 Torr), V=22.4 liter and $T_o = 273^\circ K$. Equation 2 becomes:

$$N = 6.025 \times 10^{23} \frac{\text{molecules}}{\text{mole}} \times \frac{P(mT) \times L(cm)}{\frac{760 \times 10^3 mT \times 22400 cm^3}{\text{mole}}} \times \frac{273^\circ K}{T(^\circ K)}$$

$$N = 3.539 \times 10^{13} \times PL \times \frac{273}{T} \quad (\text{molecules}/cm^2) \qquad (3)$$

using this, the yield of the recoil ions becomes:

$$Y_{m,q} = G \, \Phi_I \, \bar{\sigma}_{m,q} \, P \qquad (4)$$

where, $G = 3.539 \times 10^{13} \times L \int d\Omega \times 273/T$ (molecules/cm^2.mT). This normalization constant was obtained by measuring the yield of Ne recoil ions for Ne in the target cell at pressure P for constant experimental parameters using the cross-sections for the production of Ne recoil ions by F^{9+} (1 MeV/amu) which was measured by Gray, et al.[4] Figure 9 shows Ne spectrum produced when using F^{9+} as projectile. Since our experiment is done for different projectile species with different charge states, a gold foil and a surface barrier detector were used between the gas cell and the faraday cup to normalize for different incident projectiles using Rutherford scattering. The Rutherford scattering cross-section in laboratory coordinates is given by:

Figure 9 : Ne spectrum as a result of F^{9+} + Ne.

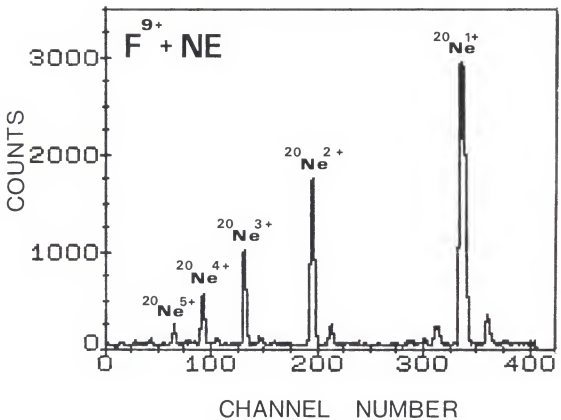
F 9+ + NE
20Ne 1+
20Ne 2+
20Ne 3+
20Ne 4+
20Ne 5+
COUNTS
3000
2000
1000
0
0
100
200
300
400
CHANNEL NUMBER

$$R^{Au}(\theta) = 1.296(Z_1 Z_2/E)^2 \left[\csc^2(\theta/2) - 2(M_1/M_2)^2 + \cdots\right] \text{mb/sr}$$

$$= K(Z_1 Z_2/E)^2 \quad , \tag{5}$$

with $\quad K = 1.296\left[\csc^2(\theta/2) - 2(M_1/M_2) + \cdots\right]$,

where, $R^{Au}(\theta)$ is the Rutherford scattering cross-section, Z_1 is the projectile atomic number, Z_2 is the target atomic number, E represents the projectile energy (MeV), and θ is the laboratory scattering angle.

The yield which is detcted by the surface barrier detector is given by:

$$Y_R^{Au} = \Phi_I \, N_{Au} \, \sigma_R^{Au} \, d\Omega_R \tag{6}$$

where, Φ_I is the total number of incident particles, N_{Au} represents the gold foil density, σ_R^{Au} is the Rutherford scattering cross-section, and $d\Omega_R$ is the solid angle of detection on the surface barrier detector.

Equation (5) and (6) give the total number of incident particles:

$$\Phi_I = \frac{Y_R^{Au}}{N_{Au}\ K(Z_1 Z_2/E)^2\ d\Omega_R} \qquad (7)$$

Using equation (4) with equation (7) we get for the Ne recoil ions

$$Y_{Ne}^{q+} = \frac{Y_R^{Au}\ E^2\ \bar{\sigma}_{Ne}^{q+}\ P_{Ne}}{Z_1^2} \left[\frac{3.539 \times 10^{13} \times L \mathcal{E}\, d\Omega}{N_{Au}\ K\ Z_2^2\ d\Omega_R} \times \frac{273}{T} \right]$$

let $$G' = \left[\frac{3.539 \times 10^{13} \times L \mathcal{E}\, d\Omega}{N_{Au} K\ Z_2^2\ d\Omega_R} \times \frac{273}{T} \right]$$

then $$G' = \frac{Y_{Ne}^{q+}}{Y_R^{Au}\ \bar{\sigma}_{Ne}^{q+}\ P_{Ne}} \times \frac{Z_1^2}{E^2} \qquad (8)$$

were we expect here the temperature T to be approximately the same when using CH_4 or Ne as the target gas.

Table 1 lists the values of G′ for the different Ne recoil ions which was measured by using equation (8) with the values[4] of $\bar{\sigma}_{Ne}^{q+}$. Taking the average of these values gives the normalization G_{Av} used in this work.

Table 1 : The values of the normalization constant for different Ne^{q+} recoil ions (q=1-4)

Table 1:

F^{9+} + Ne

q	σ_q^{Ne} (cm^2)	G
1	1.3×10^{-15}	1.98×10^{19}
2	4.5×10^{-16}	2.42×10^{19}
3	2.2×10^{-16}	2.44×10^{19}
4	1.3×10^{-16}	2.09×10^{19}
		$G_{Av} = 2.23 \times 10^{19}$

In equation (8) Y_R^{Au} is considered to be the Q-counts per channel. Then the cross-section for the production of CH_n^{q+} (q=1, n=0-4), (q=2, n=0, 1,2) when using F^{q+} as our beam, and (q=1, n=0-4), (q=2, n=0,2) when using C^{q+} and Si^{q+} as our beam, will be

$$\bar{\sigma}_{CH_n^{q+}} = \frac{Y_{CH_n^{q+}}}{(Q\text{-counts/ch})\, P_{CH_4}\, G_{Av}} \times \frac{Z_1^2}{E^2} \qquad (9)$$

E=19,12 and 28 MeV for F^{q+}, C^{q+}, Si^{q+} respectively. Table 2 presents the measured cross-sections for producing the singly-charged recoil ions CH_4^+, CH_3^+, CH_2^+, CH^+ and C^+ when bombarding CH_4 with C^{q+} projectile (q=3-6), and figure 10 represents a plot of these measured cross-sections versus the incident projectile charge state. Table 3 and 4 lists the measured cross-sections for producing the same recoil ions when bombarding CH_4 with F^{q+} (q=4,6-9), and Si^{q+} (q=6,8-12) projectiles respectively. Figures 11 and 12 display plots of these measured cross-sections versus bombarding projectile charge state. These show that the production of each charge state of recoil ions increase with increasing charge state of projectile in agreement with earlier work for the production of atomic recoil ions by Cocke[1] and Gray, et al.[4]. We observe that for different projectile ions (F^{q+},C^{q+},Si^{q+}) in the same incident charge state, the molecular ion production cross-sections are about

Table 2 : The cross sections for producing the singly charged recoil ions from CH_4 bombarded by C^{q+} (q=3-6), E=1 MeV/amu.

Table 2:

$C^{q+} + CH_4$

$\sigma_{CH_n^+}$ in units of cm^2/molecule

q	Recoil Ion				
	C^+	CH^+	CH_2^+	CH_3^+	CH_4^+
3	3.4×10^{-17}	5.9×10^{-17}	1.4×10^{-16}	8.2×10^{-16}	1.1×10^{-15}
4	8.7×10^{-17}	1.4×10^{-16}	2.9×10^{-16}	1.6×10^{-15}	1.9×10^{-15}
5	2.3×10^{-16}	3.4×10^{-16}	5.8×10^{-16}	3.0×10^{-15}	3.3×10^{-15}
6	2.6×10^{-16}	2.9×10^{-16}	5.2×10^{-16}	2.2×10^{-15}	3.3×10^{-15}

Table 3 : The cross sections for producing the singly charged recoil ions from CH_4 bombarded by F^{q+} (q=4,6-9), E=1 MeV/amu.

Table 3:

$F^{q+} + CH_4$

q	Recoil Ion				
	C^+	CH^+	CH_2^+	CH_3^+	CH_4^+
4	8.2×10^{-17}	1.1×10^{-16}	2.0×10^{-16}	7.4×10^{-16}	8.7×10^{-16}
6	2.0×10^{-16}	2.6×10^{-16}	3.7×10^{-16}	1.7×10^{-15}	2.3×10^{-15}
7	2.9×10^{-16}	2.8×10^{-16}	3.9×10^{-16}	2.0×10^{-15}	2.6×10^{-15}
8	3.7×10^{-16}	3.2×10^{-16}	4.8×10^{-16}	2.3×10^{-15}	3.0×10^{-15}
9	4.6×10^{-16}	4.0×10^{-16}	5.8×10^{-16}	2.6×10^{-15}	3.5×10^{-15}

Table 4 : The cross sections for producing the singly charged recoil ions from CH_4 bombarded by Si^{q+} (q=6,8-12), E=1 MeV/amu.

Table 4:

$Si^{q+} + CH_4$

$\sigma_{CH_n^+}$ in units of cm^2/molecule

q	Recoil Ion				
	C^+	CH^+	CH_2^+	CH_3^+	CH_4^+
6	3.2×10^{-16}	4.0×10^{-16}	6.4×10^{-16}	3.1×10^{-15}	3.5×10^{-15}
8	4.3×10^{-16}	4.2×10^{-16}	6.3×10^{-16}	2.9×10^{-15}	4.2×10^{-15}
9	5.8×10^{-16}	5.1×10^{-16}	7.5×10^{-16}	3.3×10^{-15}	4.6×10^{-15}
10	7.9×10^{-16}	7.2×10^{-16}	7.4×10^{-16}	3.7×10^{-15}	5.0×10^{-15}
11	9.9×10^{-16}	5.9×10^{-16}	8.8×10^{-16}	4.2×10^{-15}	4.6×10^{-15}
12	8.8×10^{-16}	7.4×10^{-16}	8.8×10^{-16}	4.0×10^{-15}	5.0×10^{-15}

Figure 10 : Cross-sections for producing CH_n^+ (n=0-4) for $C^{q+} + CH_4$ *vs* projectile charge state q.

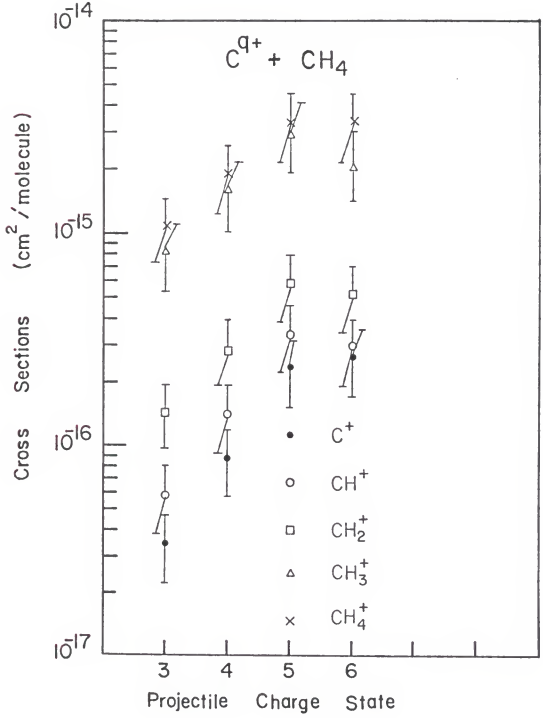
$C^{q+} + CH_4$
Cross Sections (cm^2/molecule)
10^{-14}
10^{-15}
10^{-16}
10^{-17}
C^+
CH^+
CH_2^+
CH_3^+
CH_4^+
3
4
5
6
Projectile Charge State

Figure 11: Cross-sections for producing CH_n^+ (n=0-4) for $F^{q+} + CH_4$ *vs* projectile charge state q.

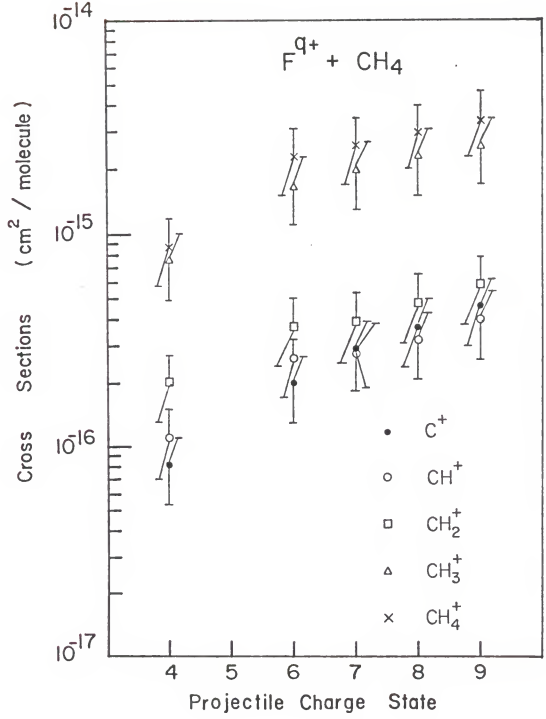
$F^{q+} + CH_4$
Cross Sections (cm^2 / molecule)
10^{-14}
10^{-15}
10^{-16}
10^{-17}
C^+
CH^+
CH_2^+
CH_3^+
CH_4^+
4
5
6
7
8
9
Projectile Charge State

Figure 12 : Cross-sections for producing CH_n^+ (n=0-4) for $Si^{q+} + CH_4$ vs projectile charge state q.

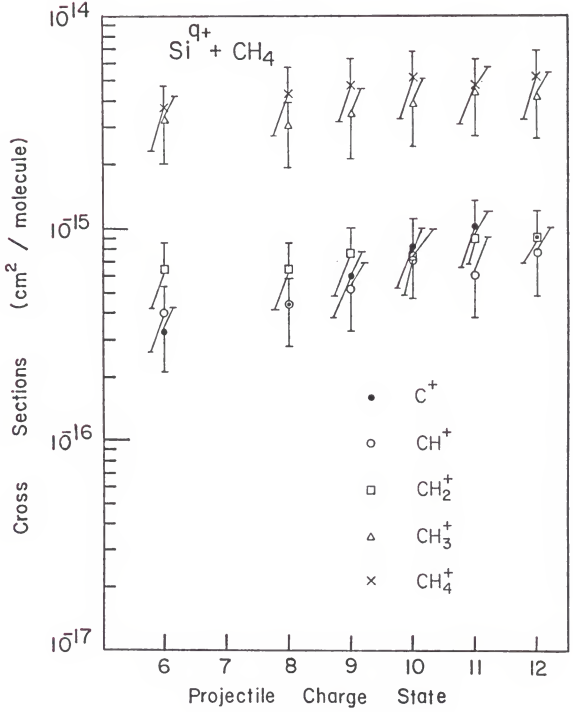
$Si^{q+} + CH_4$
Cross Sections (cm² / molecule)
10^{-14}
10^{-15}
10^{-16}
10^{-17}
C^+
CH^+
CH_2^+
CH_3^+
CH_4^+
6
7
8
9
10
11
12
Projectile Charge State

the same for a given molecular ion species. This means that we have a long range Coulomb interaction between the projectile and the target molecule, i.e the interaction is not affected by the projectile structure, but depends on the incident projectile charge state. Thus we can consider our projectiles to be point charges.

Tables 5-7 lists the cross-section for producing doubly-charged recoil ions from CH_4 with incident C^{q+}, F^{q+}, Si^{q+} fast ions, respectively. The percentage abundance of ^{13}C is 1.11% of ^{12}C, which means that 1.11% of $^{12}C^{2+}$is inseprable from CH^{2+} (M/q=6.5). Measuring CH^{2+} relative to $^{12}C^{2+}$we found that C^{q+} and Si^{q+} do not show the CH^{2+} fragement, which was very small when bombarding CH_4 with F^{q+}. This means that when using C^{q+} and Si^{q+} as the projectile beam, we dont have enough statistics tc see the CH^{2+} species.

Our measured cross-sections for the production of CH_n^{2+} recoils (n=0,1,2) versus the projectile charge states C^{q+} , F^{q+} , Si^{q+} are shown in figures 13-15 respectively.

For a comprehensive understanding of the q-dependence mechanisms of the cross-sections for producing the molecular recoil ions, the ratio $\sigma_{CH_n^+}$ / $\sigma_{CH_4^+}$ (n=0-3) and $\sigma_{CH_n^{2+}}$ / $\sigma_{CH_4^+}$ (n=0,1,2) are listed in table 8 and 9

Table 5 : The cross sections for producing the doubly charged recoil ions from CH_4 bombarded by C^{q+} (q=3-6), E=1 MeV/amu.

Table 5:

$C^{q+} + CH_4$

$\sigma_{CH_n^+}$ in units of cm^2/molecule

q	Recoil Ion	
	C^{2+}	CH_2^{2+}
3	2.1×10^{-18}	9.5×10^{-20}
4	4.1×10^{-18}	1.6×10^{-19}
5	8.8×10^{-18}	2.4×10^{-19}
6	9.5×10^{-18}	2.8×10^{-19}

Table 6 : The cross sections for producing the doubly charged recoil ions from CH_4 bombarded by F^{q+} (q=4,6-9), E=1 MeV/amu.

Table 6:

$F^{q+} + CH_4$

$\sigma_{CH_n^+}$ in units of cm^2/molecule

q	Recoil Ion		
	C^{2+}	CH^{2+}	CH_2^{2+}
4	7.2×10^{-18}	3.6×10^{-20}	2.2×10^{-19}
6	1.7×10^{-17}	6.0×10^{-20}	5.2×10^{-19}
7	2.7×10^{-17}	6.5×10^{-20}	4.1×10^{-19}
8	4.2×10^{-17}	1.4×10^{-19}	7.6×10^{-19}
9	7.1×10^{-17}	2.2×10^{-19}	8.1×10^{-19}

Table 7 : The cross sections for producing the doubly charged recoil ions from CH_4 bombarded by Si^{q+} (q=6,8-12), E=1 MeV/amu.

Table 7:

$Si^{q+} + CH_4$

$\sigma_{CH_n^+}$ in units of cm^2/molecule

q	Recoil Ion	
	C^{2+}	CH_2^{2+}
6	2.1×10^{-17}	4.3×10^{-19}
8	3.9×10^{-17}	5.4×10^{-19}
9	5.4×10^{-17}	5.0×10^{-19}
10	7.8×10^{-17}	6.9×10^{-19}
11	1.0×10^{-16}	7.7×10^{-19}
12	1.3×10^{-16}	1.1×10^{-18}

Figure 13 : Cross-sections for producing CH_n^{2+} (n=0, 2) for $C^{q+} + CH_4$ *vs* projectile charge state q.

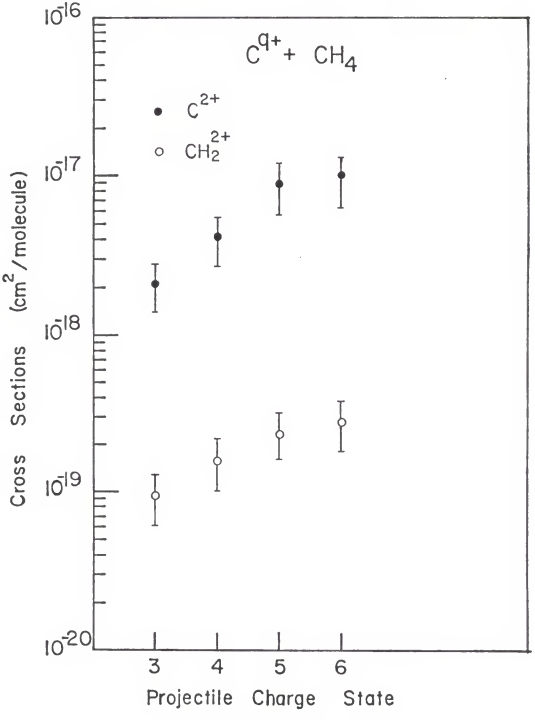
$C^{q+} + CH_4$
C^{2+}
CH_2^{2+}
Cross Sections (cm^2/molecule)
10^{-16}
10^{-17}
10^{-18}
10^{-19}
10^{-20}
3
4
5
6
Projectile Charge State

Figure 14 : Cross-sections for producing CH_n^{2+} (n=0,1,2) for F^{q+} + CH_4 *vs* projectile charge state q.

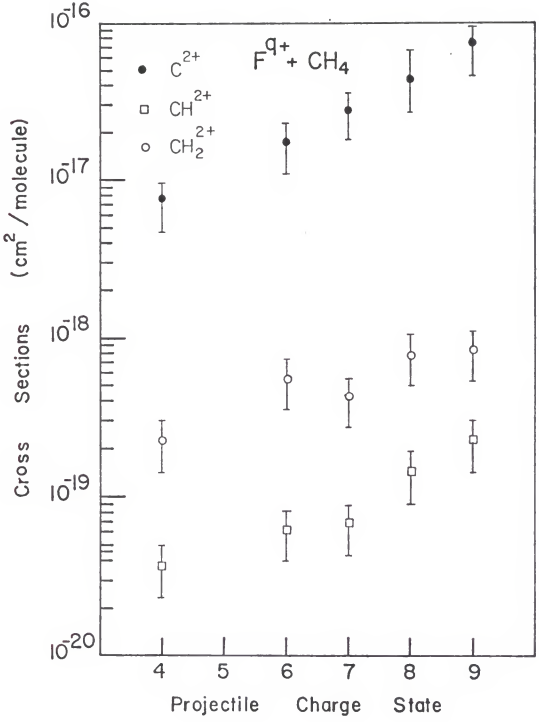
10^{-16}
10^{-17}
10^{-18}
10^{-19}
10^{-20}
Cross Sections (cm^2/molecule)
C^{2+}
CH^{2+}
CH_2^{2+}
$F^{q+} + CH_4$
4
5
6
7
8
9
Projectile Charge State

Figure 15 : Cross-sections for producing CH_n^{2+} (n=0, 2) for Si^{q+} + CH_4 vs projectile charge state q.

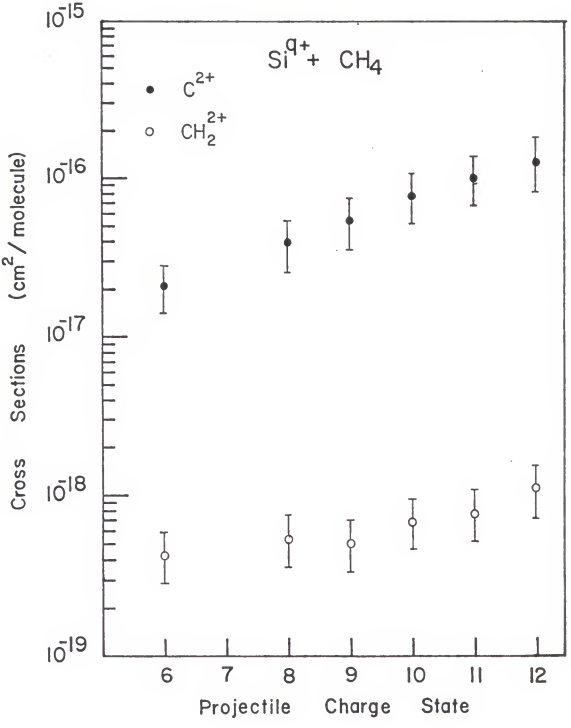
$Si^{q+} + CH_4$
C^{2+}
CH_2^{2+}
Cross Sections (cm^2/molecule)
10^{-15}
10^{-16}
10^{-17}
10^{-18}
10^{-19}
6
7
8
9
10
11
12
Projectile Charge State

respectively. The behavior of these ratios will be described in chapter 5.

Figure 16 shows the experimental cross-sections for producing CH_4^+ from methane versus q^2 (q=3-12). It is expected that calculations of the total molecular ion production cross-section by fast heavy ions based upon the first Born approximation are adequate when q is small and the velocity v of the projectile ion is large. But in this experiment we consider some large values of q at high velocity, which means that we may expect a breakdown of the Born approximation at some large q. It was suggested by McGuire[18] that for high velocity projectiles, the Glauber approximation gives better agreement with the experimental molecular ion production cross-section $\sigma_{CH_4^+}$ than the simpler Born approximation calculations. To verify this, McGuire[18] provided theoretical calculations for $\sigma_{CH_4^+}$ using both the Born and Glauber approximations. The molecule CH_4 was approximated by 4 hydrogen atoms with variable binding energy u, and atomic radius r. The choice of $r=a_0$ (Bohr radius) and u=13.6 eV was used in figure 16 where the Born and Glauber calculations are compared to our measured q-dependence of single ionization of CH_4 yielding CH_4^+. While both approximations predict the measured trend in the experimental data, the Glauber approximation is in closer

Table 8 : The ratios $\sigma_{CH_n^+} / \sigma_{CH_4^+}$ (n=0-3)

Table 8 : $\left(\bar{\sigma}_{CH_n^+} / \bar{\sigma}_{CH_4^+}\right) \times 100$

	12/16	13/16	14/16	15/16
F^{9+}	13.3	11.5	16.8	75.0
F^{8+}	12.3	10.6	16.0	74.3
F^{7+}	11.0	10.7	15.3	76.7
F^{6+}	8.8	11.5	16.5	73.1
F^{4+}	9.4	12.0	23.0	87.0
Si^{12+}	18.6	14.8	17.6	80.0
Si^{11+}	21.7	12.8	19.1	91.3
Si^{10+}	15.8	14.4	14.8	72.0
Si^{9+}	12.6	11.1	16.3	71.7
Si^{8+}	10.2	10.0	15.0	69.0
Si^{6+}	9.1	11.4	18.0	88.0
C^{6+}	7.9	8.8	15.8	63.6
C^{5+}	7.0	10.3	17.6	90.9
C^{4+}	4.6	7.4	15.3	84.2
C^{3+}	3.1	5.4	12.7	74.5

Table 9 : The ratios $\bar{\sigma}_{CH_n^{2+}} / \bar{\sigma}_{CH_n^{+}}$ (n=0,1,2)

Table 9 : $\left(\sigma_{CH_n^{2+}} / \sigma_{CH_4^+}\right)$ x 100

	6/16	6.5/16	7/16
F^{9+}	2.1	6.4×10^{-3}	0.020
F^{8+}	1.4	4.7×10^{-3}	0.030
F^{7+}	1.1	2.5×10^{-3}	0.020
F^{6+}	0.8	2.6×10^{-3}	0.020
F^{4+}	0.8	4.1×10^{-3}	0.030
Si^{12+}	2.5	----	0.022
Si^{11+}	2.2	----	0.017
Si^{10+}	1.6	----	0.014
Si^{9+}	1.2	----	0.011
Si^{8+}	0.9	----	0.013
Si^{6+}	0.6	----	0.012
C^{6+}	0.3	----	0.009
C^{5+}	0.3	----	0.007
C^{4+}	0.2	----	0.008
C^{3+}	0.2	----	0.009

Figure 16 : Experimental and theoretical calculations of the cross sections for producing CH_4^+ from methane vs q^2 (q=3-12)

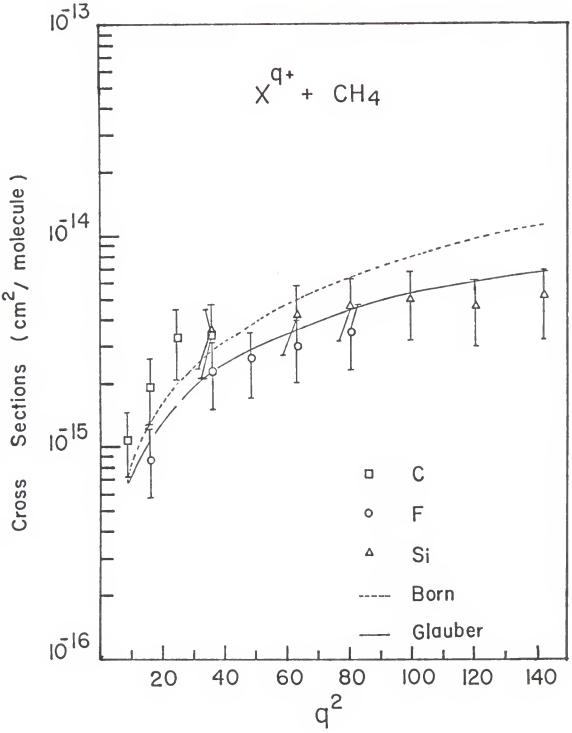
$X^{q+} + CH_4$
Cross Sections (cm^2 / molecule)
10^{-13}
10^{-14}
10^{-15}
10^{-16}
20
40
60
80
100
120
140
q^2
C
F
Si
Born
Glauber

agreement with the mesurements.

In figure 17, a plot of the ratios $\sigma_{CH_n^+} / \sigma_{CH_4^+}$ (n=0-3) are shown as a function of q, while figure 18 shows the same ratio versus the velocity v of the projectile when using H^+ on CH_4 (1MeV).

The experimental uncertainty to which we normalize our data was about 20%, and as we discussed in chapter 3 the reproducibility was $\lesssim$ 10% and $\sim$ 5% due to the dead time loses for the highest peak in the spectrum. These together with the statistical errors in the area measured gives an error bars in our results of the cross-section of about 35%.

Figure 17 : The ratios $\sigma_{CH_n^+}$ / $\sigma_{CH_4^+}$ vs q (q=1-12), (n=0-3).

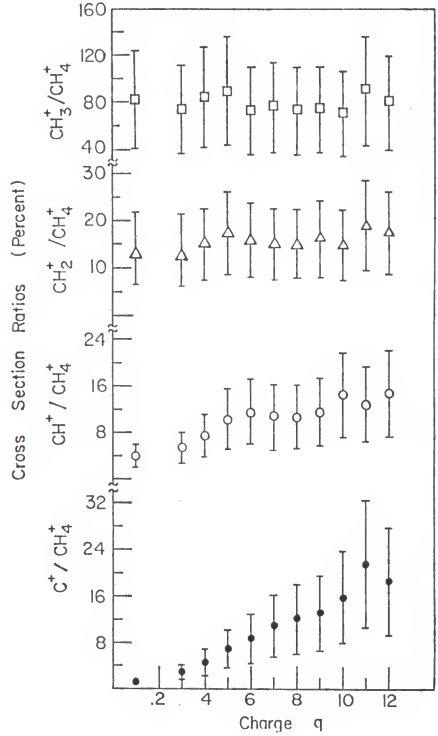
Cross Section Ratios (Percent)
C^+/CH_4^+
CH^+/CH_4^+
CH_2^+/CH_4^+
CH_3^+/CH_4^+
Charge q

Figure 18 : The ratios $\bar{\sigma}_{CH_n^+} / \bar{\sigma}_{CH_4^+}$ vs the velocity of the projectile v, for $H^+ + CH_4$,E=(1.0-11.0)MeV.

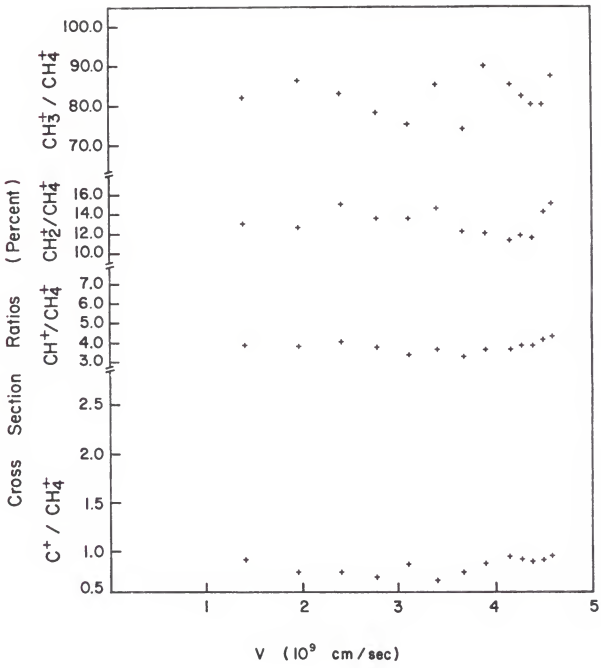
Cross Section Ratios (Percent)
C+ / CH4+
CH+/CH4+
CH2+/CH4+
CH3+ / CH4+
100.0
90.0
80.0
70.0
16.0
14.0
12.0
10.0
7.0
6.0
5.0
4.0
3.0
2.5
2.0
1.5
1.0
0.5
1
2
3
4
5
V (10^9 cm/sec)

Figure 19: The ratios $\sigma_{CH_n^{2+}} / \sigma_{CH_4^+}$ vs q (q=3-12), (n=0-2).

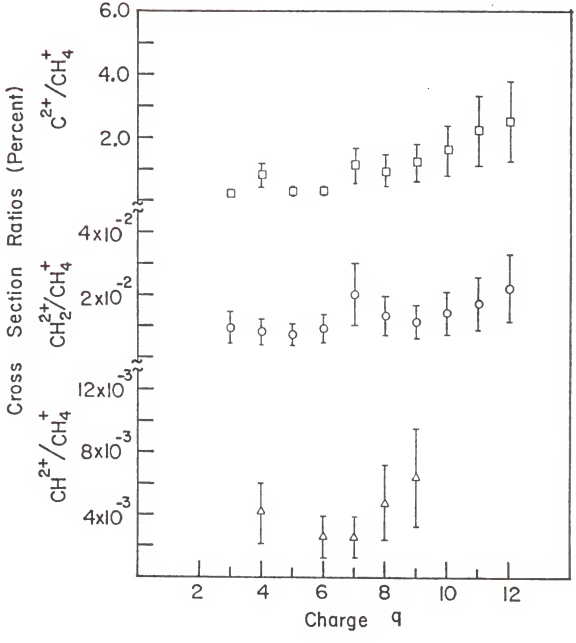
Cross Section Ratios (Percent)
C^{2+}/CH_4^+
CH_2^{2+}/CH_4^+
CH^{2+}/CH_4^+
6.0
4.0
2.0
$4x10^{-2}$
$2x10^{-2}$
$12x10^{-3}$
$8x10^{-3}$
$4x10^{-3}$
2
4
6
8
10
12
Charge q

CHAPTER FIVE

SUMMARY AND CONCLUSION

In the present work, a systematic experimental study of the product of a single collision of a fast highly ionized heavy projectiles with CH_4 gas has been conducted. The cross-sections for the production of low energy recoil molecular ions with different projectiles bombarding CH_4, in a recoil ion source, were measured.

The experimental results of the present work for the production cross-sections for CH_4^+ molecule by fast heavy ions incident upon CH_4 were compared with theoretical calculations[18] using the Glauber and first Born approximations. This comparison for the production of CH_4^+ can be seen in figure 16. The Glauber calculations are in better agreement with our measurements than the first Born calculations. The agreement between theory and experiment suggests that the cross-section dependence upon incident projectile charge state, q, for producing CH_4^+ is of the form q^n, where $n \lesssim 2$. We conclude that CH_4^+ is produced by direct Coulomb interaction with the projectile as is discussed later in this chapter.

Returning to figure 17 we notice the following:

(1)The ratio $\sigma_{CH_n^+} / \sigma_{CH_4^+}$ (n=2,3) for C^{q+}, F^{q+}, and Si^{q+} projectiles is independent of the incident projectile charge state in the range q=3-12.

(2)But for the other data in this figure, we notice that the ratio increases with q but not faster than q^2.

Same results for doubly charged recoil ions CH_n^{2+}, are shown in figure 19. These are the first direct observations of multiply charged molecular ions fragments.[17] It is not clear that the projectiles may be regarded as point particles of charge q in these cases. The trends of the fragmentation ratios of CH_n^{2+} to CH_4^+ are not inconsistent with the singly charged data above.

The physical interpretations for the above observations were suggested by McGuire[18]. Consider two distinct types of ionization mechanisms:

(a)Final State Rearrangement (R) Mechanisms:[19,20]

McGuire suggested that in the $X^{q+} + CH_4$ collision, ion fragments other than CH_4^+ are produced when the electronic cloud of the target molecule readjusts after production of CH_4^+ by direct Coulomb interaction with the

incident charged particle. Following the initial interaction of the projectile with CH_4 , the exited CH_4^+ ion dissociates to form other molecular ion species, i.e CH_3^+ , etc. The resulting molecular ions are assumed to be the result of post interaction rearrangement (R) occurring in the final state parent ion. This R mechanism is due to electron-electron correlation in the target wave function and is often referred to as rearrangement (or shake-off). In the R mechanism the ratio $\sigma_{CH_n^+} / \sigma_{CH_4^+}$ is independent of the charge q and the velocity v of the projectiles as illustrated in figures 17 and 18 respectively. Figures 17 and 18 show that, CH_3^+ , CH_2^+ , and possibly CH^+ are produced in a shake-off mechanisms. The data for CH^+ versus q does exhibit a slight q-dependence suggesting that a mechanism other than R is also contributing to the formation of CH^+ in the initial collision.

(b)Direct Collision Mechanisms (D):[19,20]

McGuire also suggested that an increasing dependence of the fragmentation ratios on q could be described by the D mechanisms which corresponds to dissociation of the molecule via direct Coulomb interaction with the projectile ion. In the D mechanism the fraction of $\sigma_{CH_n^+} / \sigma_{CH_4^+}$(n=0,1,2 or 3) varies as q^m, m>2 at high velocities. This means that the cross -sections in this

mechanism are approximately described by the second Born approximation or $\sigma_{CH_n^+} \sim q$, where $\sigma_{CH_4^+} \sim q^n$, $n \lesssim 2$.

We note that in theory the R mechanism is dominant over the D mechanism at sufficiently high energies or high velocity where the simple Born or Glauber approximation plus rearrangement works.

Further more, in the D mechanism the fragmentation ratios are predicted to decrease with increasing v, e.g as v^{-2}. Experimental tests of this prediction are now in progress.

Figure 17 show that $\sigma_{C^+} / \sigma_{CH_4^+}$ varies as q or possibly q^2. Since this ratio increases with q, this suggests that the D mechanism is significant. We note that interference between R and D mechanisms can be linear in q at high velocities.

Wexler's test of the Born approximation in molecular ion production by protons corresponds to our idea of the "R mechanism" with the first Born approximation. He found that the production of both CH_4^+ and CH_3^+ obeys the simple Born approximation but this was not the case for the CH_2^+ ,CH^+ , and C^+.

No clear explanation for the decrease in the magnitude of the molecular production cross-section between CH_3^+ and CH_2^+ has been found yet. This is an area in need of additional investigation both from experimental and especially theoretical points of view.

It was found that the cross sections for the singly charged molecular ions are as large as $5 \times 10^{-15} cm^2$ for producing CH_4^+ for $Si^{12+} + CH_4$, and remain at least of the order of $10^{-16} cm^2$ for the incident projectile charge state 6 for the same target when producing C^+ recoil ion. These large cross-sections, together with the high extraction efficiency using the 180° magnetic spectrometer, leads us to believe that it is possible to use these recoil ions as projectiles in a further experiments for the studies of ion-neutral target reaction.

Using the time-of-flight technique Needham[17] gave an estimate of values for the lifetime of some of the recoil ions produced from methane, it might be feasible in the future to conduct an experiment for measuring lifetime for these recoils using the magnetic spectrometer with a new recoil ion source for better time resolution.

REFERENCES

1) C. L. Cocke, Phys. Rev. A203 (1979) 749.

2) R. Mann, C. L. Cocke, A. S. Schlachter, M. Prior and R. Marrus, Phys. Rev. Lett. 49, (1982) 1324.

3) A. S. Schlachter, W. Groh, A. Muller, H. F. Beyer, R. Mann and R. E. Olson, Phys.Rev. A26 (1982) 1373.

4) T. J. Gray, C. L. Cocke and E. Justiniano, Phys. Rev. A2 (1980) 849.

5) P. Richard, I. L. Morgan, T. Furuta, and D. Burch, Phys. Rev. Lett. 23 (1969) 1009.

6) R. D. Macfarlane and D. F. Torgerson, Phys. Rev. Lett. 36 (1976) 48.

7) A. K. Edwards, R. M. Wood and M. F. Stever, Phys. Rev. A15 (1977) 48.

8) Lincoln G. Smith, Phys. Rev. 51 (1937) 263.

9) S. Wexler, J. Chem. Phys. 41 (1964) 2781.

10) Rowland I. Reed, "Modern Aspects of Mass spectrometry" (Plenum Press. New York, 1968) pp.255.

11) B. Adamczyk, A. J. H. Boerboom, B. L. Schram, and J. Kislemaker, J. Chem. Phys. 44 (1966) 4640.

12) R. Spohr, T. Bergmark, N. Magnusson, L. O. Werme, C. Nordling and K. Siegbahn, Phys. Scripta 2 (1970) 31.

13) T. Ast, C. J. Porter, C. J. Proctor, and J. H. Beynon, Chem. Phys. Lett. 79 (1981) 439.

14) M. Rabrenovic, A. G. Brenton, and J. H. Beynon, Int. Journal Mass Spect. Ion Phys. 52 (1983) 175.

15) T. J. Gray, J. C. Legg, and Vincent Needham, Nuclear Instruments and Methods in Physics Res. (1985) 253.

16) T. J. Gray, and C. L. Cocke, IEEE Trans. Nucl. Sci. 30 (1983) 937.

17) Vincent Needham, M.S. Thesis (Kansas State University, 1984).

18) J. McGuire, Private Communications.

19) J. McGuire, A. Muller, B. Schuch, W. Groh, and E. Salzborn, "Ionization of He by Highly Charged Ions at 1.4 MeV/amu",To be Published.

20) J. McGuire, 2nd U.S. Mexico Symposcum on Atomic Physics, Jan.86 Cocoyoc Mexico.

CROSS SECTIONS FOR PRODUCING MOLECULAR IONS FROM METHANE FOR FAST F, Si, AND C PROJECTILES

by

NABIL B. MALHI

B.S.,UNIVERSITY OF JORDAN, AMMAN/ JORDAN, 1980

M.S.,UNIVERSITY OF JORDAN, AMMAN/ JORDAN, 1982

AN ABSTRACT OF A MASTER'S THESIS

submitted in partial fulfillment of the

requirements for the degree

MASTER OF SCIENCE

Department of Physics

Kansas State University

1986

ABSTRACT

Measurements of the production cross sections for singly and doubly charged molecular ions produced by fast heavy ion bombardment of CH_4 introduced into a recoil ion source have been done. The cross sections have been measured for F, Si, and C projectile ions with the energy 1 MeV/amu. Measurements have shown that cross sections for producing CH_n^{q+} for the projectile charge state range 3-12 to be dependent on the projectile ion charge state and not on the projectile species.